Metabolism of Thiazopyr in Laying Hens

William P. Ridley,*,† Hideji Fujiwara,† Theresa Cheng,‡ and Joy L. Honegger†

Agricultural Sector, Monsanto Company, 700 Chesterfield Parkway North, St. Louis, Missouri 63198, and Covance, 3301 Kinsman Boulevard, Madison, Wisconsin 53704

Thiazopyr labeled with $^{13}C/^{14}C$ was found to be rapidly metabolized and eliminated by laying hens dosed orally for four consecutive days at either 1.3 or 10.4 mg/day. Over 90% of the total radioactive dose appeared in the excreta within 22 h after the final dose at both levels. Tissue residues were very low in the muscle and egg white (0.004−0.01 ppm) with somewhat higher levels observed for the liver, abdominal fat, skin with fat, egg yolk, and kidney (0.047−0.298 ppm). The most abundant tissue metabolite was a nitrile ester resulting from the breakdown of the thiazoline ring of thiazopyr. A carboxylic acid metabolite found in the liver and excreta was shown to arise from oxidation at C-3 of the isobutyl side chain of the nitrile ester. In vitro liver homogenate studies demonstrated the presence of similar metabolic pathways in hens, goats, and rats, although the levels of individual metabolites varied.

Keywords: *Thiazopyr; hens; metabolites; MS; NMR*

INTRODUCTION

Thiazopyr [methyl 2-(difluoromethyl)-5-(4,5-dihydro-2-thiazolyl)-4-(2-methylpropyl)-6-(trifluoromethyl)-3-pyridinecarboxylate] (see **1** in Figure 1) is a herbicide developed for weed control in cotton, citrus, and other crops. Reports in the literature (Armbruster et al., 1988, 1991) suggest that disruption of cell division via inhibition of microtubule formation is the mode of action of this class of pyridine compounds.

The metabolism of thiazopyr has been extensively studied in animals (Klemm et al., 1993; Feng et al., 1994, 1995a; Feng and Solsten, 1994; McClanahan et al., 1995) and plants (Feng et al., 1995b; Rao et al., 1995). Four major pathways have been identified—C-oxidation, S-oxidation, O-demethylation, and ester hydolysis. The relative contribution of an individual pathway has been shown to vary with the animal or plant species being studied. In liver microsomes from Long Evans rats the metabolites of thiazopyr resulted primarily from C- and S-oxidation of the thiazoline ring (Feng et al., 1994). Similar studies using liver microsomes from Sprague−Dawley rats demonstrated the presence of oxidative cleavage of the carboxylic ester of thiazopyr catalyzed by monooxygenases (Feng and Solsten, 1994). Animal and plant esterases have also been shown to degrade the methyl ester group of thiazopyr to give a monoacid metabolite that showed <1% of the herbicidal activity of the parent (Feng et al., 1995a).

In this study we describe the identity and distribution of thiazopyr residues in the eggs, tissues, and excreta of laying hens. Because livestock may consume thiazopyr on treated foodstuffs, it was important to determine its metabolic fate in a representative livestock species. In addition, we have compared the in vitro metabolism of a key thiazopyr metabolite (**2** in Figure 1) using liver homogenates from hens, goats, and rats. A pathway has been proposed to account for the observed in vivo and in vitro metabolites.

MATERIALS AND METHODS

Chemicals. [^{14}C]- and [^{13}C]thiazopyr labeled in the C-4 position of the pyridine ring (Figure 1) was prepared by custom synthesis at Monsanto Co., St. Louis, MO. Appropriate amounts of [^{12}C]-, [^{13}C]-, and [^{14}C]thiazopyr were combined to produce test substances with specific radioactivites of 7.93 (high dose) and 16.14 mCi/mmol (low dose). The ^{13}C enrichment in both test substances was 50%, giving rise to a readily discernible pattern in the mass spectrum. Chemical purities were a minimum of 97.7%, and radiochemical purities were >96%. Authentic standards for metabolites **2** and **7** (see Figure 1) were furnished by the Monsanto Sample Retention Center. Atomlight and Atomflow liquid scintillation cocktails were obtained from NEN Products, Boston, MA, and all other reagents and solvents were obtained from commercial suppliers.

Preparation of Dosing Capsules. Labeled thiazopyr was dissolved in acetonitrile, portions were transferred to gelatin capsules, and the acetonitrile was evaporated under a gentle stream of nitrogen. The capsules were sealed and then stored frozen until dosing. At selected times before, during, and after dosing, capsules were extracted with acetonitrile and analyzed for total radioactivity and radiochemical purity by HPLC. Thiazopyr was shown to be stable for up to 7 days (average recovery was 97.4%, $n = 3$) when stored in this manner.

Animal Handling and Dosing. Single-comb White Leghorn laying hens were obtained from S&R Egg Farm (Whitewater, WI). The birds were 25−32 weeks of age upon receipt and weighed ∼1400−1600 g each. Hens were selected from a pool of birds based upon egg production (average egg production/hen/day = 0.975) during an acclimation period and randomly assigned by body weight to a test group with five hens per group. Labeled thiazopyr was administered orally in gelatin capsules via a balling gun once daily for four consecutive days. Groups 1 and 2 received an average of 1.3 mg of thiazopyr/day (low dose), which exceeded the maximum potential dietary exposure in feed by more than an order of magnitude. Two low-dose groups were treated to provide

* Author to whom correspondence should be addressed [telephone (314) 737-6241; fax (314) 737-6134; e-mail william.p.ridley@monsanto.com].

† Monsanto Co.

‡ Covance.

10.1021/jf9802833 CCC: $15.00
Published on Web 09/25/1998

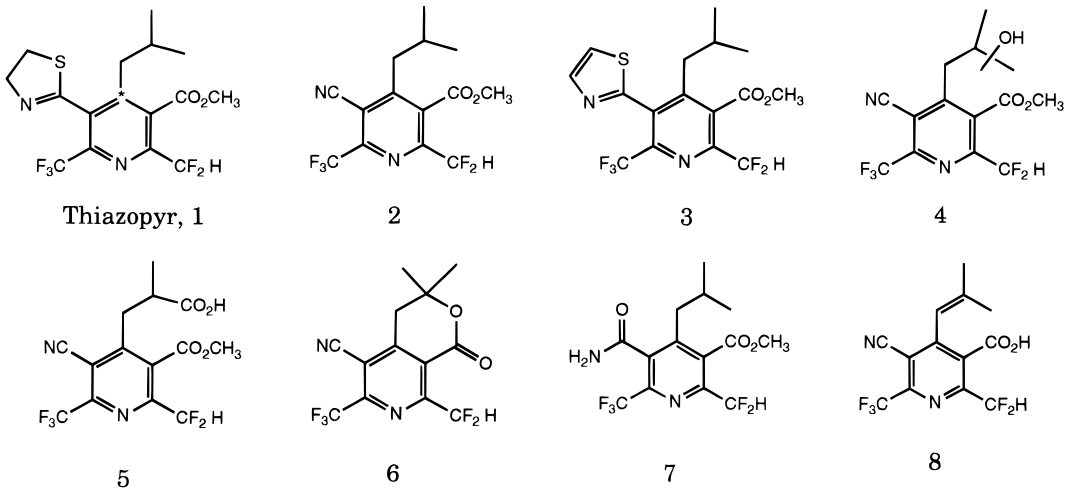

Figure 1. Structures of thiazopyr and its metabolites. The asterisk (*) denotes the site for $^{13}C/^{14}C$ labeling of thiazopyr.

additional tissue for metabolite isolation. A high-dose group (group 3) received 10.4 mg/day and was included to provide sufficient quantities of low-level metabolites for identification. On the basis of actual food consumption during the study, the low-dose groups received the equivalent of 12 μg of thiazopyr/g (ppm) of diet and the high-dose group received 78 ppm. An additional group of hens was treated with placebo capsules and served as a source of control tissue.

Sample Collection and Analysis. Eggs were collected twice daily in the morning and evening. The evening eggs were stored refrigerated and then added to the morning collection the following day. After collection, the eggs were separated into yolks and whites and stored separately in glass jars at −20 °C. Excreta samples were collected once daily from Teflon-coated paper that was placed below the cages of each group. All samples were pooled according to day, sample matrix, and group and then frozen. Approximately 22 h after the last dose, the hens were anesthetized with carbon dioxide, a sample of blood was collected in heparinized tubes by cardiac puncture, and the birds were sacrificed by carbon dioxide overdose. Tissue samples were taken from each animal upon necropsy, and each tissue type was pooled by treatment group. Tissues collected were liver, abdominal fat, skin with fat, kidneys, thigh muscle, and breast muscle. Eggs and tissues were homogenized, and aliquots solubilized or combusted for radiochemical analysis. Excreta were homogenized with water and centrifuged, and aliquots of the supernatant and the centrifugation pellet were taken for radiochemical analysis.

Metabolite Extraction and Isolation. Tissues (35−150 g) from low-dose groups 1 and 2 containing ≥0.01 μg of thiazopyr equiv/g were extracted and analyzed for metabolites. Egg yolk, liver, abdominal fat, and skin with fat were isolated from group 2, whereas a pooled sample from both low-dose groups was used for kidney and thigh muscle analysis. The high-dose (group 3) excreta and abdominal fat were also used for metabolite isolation.

A portion of the fourth day excreta sample (58.9 g) was extracted two times with 50 mL of acetonitrile/water (70:30), the extracts were combined, and the metabolites were partitioned into an equal volume of ethyl acetate. The remaining aqueous phase was adjusted to contain 1% aqueous formic acid and extracted with an equal volume of ethyl acetate. The ethyl acetate extracts were combined and concentrated to near dryness, and the residue was dissolved in 20 mL of 1% formic acid/methanol (1:1). The reconstituted residue was applied to a 10 g C-18 Mega-Bond Elut solid-phase extraction column (Varian Associates Inc., Harbor City, CA) and rinsed with 50 mL of 1% formic acid/methanol (1:1), and purified metabolites were eluted with 50 mL of methanol.

A portion of the fourth day egg yolk sample (54.8 g) was extracted two times with 30 mL of acetonitrile and then once with an equivalent volume of acetonitrile/water (70:30). The extracts were concentrated to remove the acetonitrile, adjusted to contain 1% formic acid, and applied to a 10 g C-18 Mega-Bond Elut column. The column was rinsed with 50 mL of 1% formic acid, and metabolites were eluted with methanol. The methanol solution was concentrated and mixed with an equal volume of 1% formic acid, and the metabolites were isolated by HPLC or partitioning into methylene chloride. The methylene chloride solution was dried over sodium sulfate concentrated to near dryness and the residue dissolved in 1% formic acid/methanol.

A 110 g liver sample was extracted two times with 50 mL of acetonitrile/water (70:30) and once with acetonitrile/0.1 N HCl using a Tissuemizer (Tekmar Co., Cincinnati, OH) to grind and mix the sample. The residue was extracted for 16 h with 250 mL of acetonitrile/water (60:40) using a Soxhlet apparatus (Fisher Scientific, St. Louis, MO). The extracts were combined, concentrated, and purified using a C-18 Mega-Bond Elut column and the procedure followed for the egg yolk.

Abdominal fat and skin with fat samples (57 g) were extracted two times with 25 mL of acetonitrile, concentrated to ∼1 mL, and mixed with an equal volume of 1% formic acid. The kidney (34.8 g) and thigh muscle (150 g) were extracted two times with acetonitrile/water (70:30), and the kidney was extracted one additional time with acetonitrile/0.1 N HCl, followed by concentration to remove acetonitrile.

Combustion and Liquid Scintillation Counting. Replicate combustions (3−12, 0.1−0.5 g) were performed using a Packard Tri-Carb automatic sample oxidizer model B306 (Packard Instrument Co., Downers Grove, IL). Performance of the oxidizer was monitored daily by combustion of a C-14 standard or fortification of control tissue with a C-14 standard. The average recovery for C-14 standards was >97%. Liquid scintillation counting was performed with a TM Analytic Mark III model 6881 or Packard Tri-Carb models 1500 or 4640 counters using automatic external standard efficiency correction. An estimation of the sensitivity of the method was calculated as 0.002 ppm for groups 1 and 2 and 0.004 ppm for group 3, assuming a sample contained 34 dpm above background and a typical aliquot weight of 0.2 g was combusted.

High-Performance Liquid Chromatography (HPLC). The HPLC system consisted of the following components: a Waters model U6K injector (Waters Associates, Milford, MA); two Waters model 510 pumps; a Waters 484 tunable absorbance detector (operated at 254 nm); and a Waters 680 automated gradient controller. The effluent was passed through a Flo-One Beta radioactive flow detector (Packard Instrument Co.) equipped with a 2.5 mL liquid cell or 250 μL solid cell. A Beckman Ultrasphere ODS 5 μm (10.0 mm × 25 mm) column (Beckman Instruments Inc., San Ramon, CA) equipped with a Brownlee PRP-1 or RP-18 Newguard column (15 mm × 3.2 mm) (Applied Biosystems, Inc., Foster City, CA) was used. The profiling HPLC gradient was conducted in linear steps at a flow rate of 3 mL/min, utilizing 1% formic acid (solvent A) and methanol (solvent B). The gradient

proceeded from 50% B to 63% B over 18 min, remained at 63% B for 12 min, proceeded to 70% B over 2 min, remained at 70% B for 18 min, proceeded to 100% B over 5 min, and then remained at 100% B for an additional 5 min. The effluent from the column was mixed with Atomflow pumped at 9 mL/min and collected in vials at 0.3 min intervals with an ISCO fraction collector (Retriever III, Instrument Specialties Co., Lincoln, NE).

Mass Spectrometry (MS) and Nuclear Magnetic Resonance (NMR) Spectroscopy. Chemical ionization (CI) mass spectra were obtained using a Finnigan 4515 quadrupole mass spectrometer and processed with a Data General Nova 4 computer using INCOS software. The samples were introduced using a Finnigan 9610 gas chromatograph that was equipped with a J&W Scientific DB-5 capillary column (25 m × 0.32 mm) and programmed between 70 and 300 °C. Helium was used as the carrier gas at a flow rate of 2 mL/min. Chemical ionization of the gas chromatograph effluent was performed using isobutane (0.5 Torr). Negative and in some cases positive ions were analyzed.

Fast-atom bombardment (FAB) mass spectra and high-resolution FAB analyses were recorded on a VG ZAB-HF double-focusing mass spectrometer and processed with a DEC PDP 11/24 data system (Maynard, MA). The samples were deposited on a thin layer of glycerol and then introduced into the mass spectrometer by direct probe. Microbore liquid chromatography (LC) FAB mass spectra were obtained by introducing the sample using an microbore HPLC system that consisted of an Applied Biosystems Inc. (Santa, Clara, CA) model 140A syringe pump, a Brownlee C-18 column (1 × 250 mm), and a VG (Manchester, U.K.) dynamic FAB/MS probe. Ionization was achieved for all FAB analyses with an Ion Tech Saddle Field fast atom gun (Middlesex, U.K.) producing 7 kV xenon atoms at 1 mA emission current. Negative ions were analyzed.

^{1}H NMR spectra were obtained using a Varian XL-300 spectrometer with a proton operating frequency of 300 MHz. Chemical shifts were referenced using the resonance frequency of the solvent peak through the Monsanto Switch software package, a proprietary automated expert system, and are reported in parts per million from tetramethylsilane. Samples were dissolved in high-purity deuteriochloroform and placed in 5 mm tubes (Wilmad Glass Co., Buena, NJ). ^{19}F NMR spectra were also obtained using a Varian XL-300 NMR spectrometer. Two-dimensional correlation spectroscopy (2-D COSY) was performed using a Varian XL-500 NMR spectrometer.

Diazomethane Derivatization. Methyl esters of carboxylic acids were prepared by extracting the purified metabolites from the HPLC mobile phase with methylene chloride, concentrating to near dryness, and dissolving in 1−2 mL of diethyl ether. Etheral diazomethane was added until the yellow color persisted, and then the solution was incubated at room temperature for 10 min. Solvent and excess reagent were removed with a stream of nitrogen, and then the sample was dissolved in acetonitrile or methanol prior to MS analysis.

Liver Homogenate Preparation and Incubation Conditions. Approximately 100 g of liver tissue from control hens, male rats (Sprague−Dawley, 200−250 g body weight), and a control lactating goat (Sunshine Farms, Portage, WI; 60 kg body weight) was chilled on ice and homogenized with 0.01 M potassium phosphate buffer, pH 7.4, containing 1.15% KCl at a tissue-to-buffer ratio of 1:3 (w/v) using a Potter−Elvehjem homogenizer or a Tissumizer (Tekmar Co., Cincinnati, OH). Homogenates were centrifuged at 4 °C for 30 min at 9000*g*, filtered through gauze to remove lipids, aliquoted, and stored at −70 °C until used.

Metabolite **2** was isolated from the abdominal fat of group 3, and its metabolism by liver homogenates was studied in a reaction containing 10 mM glucose 6-phosphate, 5 mM nicotinamide, 5 mM magnesium chloride, 1.3 mM $NADP^+$, 10 units of glucose-6-phosphate dehydrogenase, 11.3 mg of liver homogenate, and 0.2 M potassium phosphate buffer, pH 7.4, in a total volume of 0.985 mL. Components were preincubated at 37 °C for 5 min, and then the reaction was started by the addition of 15 μL of a methanol solution of metabolite **2**, which gave a final concentration of 4.0−5.0 μM. The reaction containing hen homogenate was incubated for 3 h at 37 °C, stopped by the addition of 1.0 mL of cold methanol, and then stored at −20 °C until analyzed. The reactions with goat and rat liver homogenates were identical to the hen except that they were incubated for 2 h at 37 °C.

Table 1. Distribution of Radioactivity in Eggs, Excreta, and Tissues of Hens Dosed with [^{14}C]Thiazopyr

	% of total radioactive dose		
matrix	group 1 (1.3 mg/day)	group 2 (1.3 mg/day)	group 3 (10.4 mg/day)
egg white	0.02	0.02	0.02
egg yolk	0.03	0.04	0.05
excreta	94.31	90.08	92.73
tissues[a]	0.43	0.62	0.49
total	94.79	90.76	93.29

[a] Consists of gastrointestinal tract, liver, kidneys, and the portions of abdominal fat, skin with fat, thigh muscle, and breast muscle taken at necropsy.

Table 2. Total Radioactive Residues in Egg White, Egg Yolk, and Tissues at Sacrifice

	μg equiv of thiazopyr/g of sample[a] (ppm)		
sample	group 1 (1.3 mg/day)	group 2 (1.3 mg/day)	group 3 (10.4 mg/day)
liver	0.222	0.298	1.112
abdominal fat	0.123	0.173	1.417
skin with fat	0.049	0.097	0.488
egg yolk	0.077	0.075	0.626
kidneys	0.047	0.052	0.501
blood	0.016	0.021	0.097
egg white	0.008	0.008	0.052
thigh muscle	0.010	0.008	0.086
breast muscle	0.004	0.005	0.033

[a] Specific activities of 87950 (for groups 1 and 2) and 44420 (for group 3) dpm/μg equiv of thiazopyr were used to calculate ppm.

RESULTS

Distribution of Total Radioactivity. The total recovery of radioactivity in the samples of eggs, excreta, and tissues collected for analysis from groups 1−3 is summarized in Table 1. The total recovery of administered dose ranged from 90.8 to 94.8% with a majority of the radioactivity (90.1−94.3%) eliminated in excreta. The entire egg production contained <0.1% of the total dose, and all analyzed tissues accounted for <1% of the total dose.

Nature of Residues in Eggs, Excreta, and Tissues. A summary of the concentration of thiazopyr-derived residues in the eggs and tissues is shown in Table 2. The residues were very low (≤0.01 ppm) for the muscle and egg white following dosing at 1.3 mg/day (groups 1and 2). The highest levels of residues were found in the liver and abdominal fat for groups 1 and 2 and varied between 0.123 and 0.298 ppm. All other tissue residues were <0.1 ppm. The data for the two low-dose groups (1 and 2) were in close agreement and, in general, the residue levels of the tissues from the high-dose group (group 3) were proportionally higher than those for the low-dose groups.

Portions of the tissues and excreta were extracted as described under Materials and Methods. Total extractability varied from 71.6% of the radioactive residue for the kidney to 94.1% for the thigh muscle. Total accountability of radioactive residue averaged 103.6% for the tissues and 78.5% for the excreta.

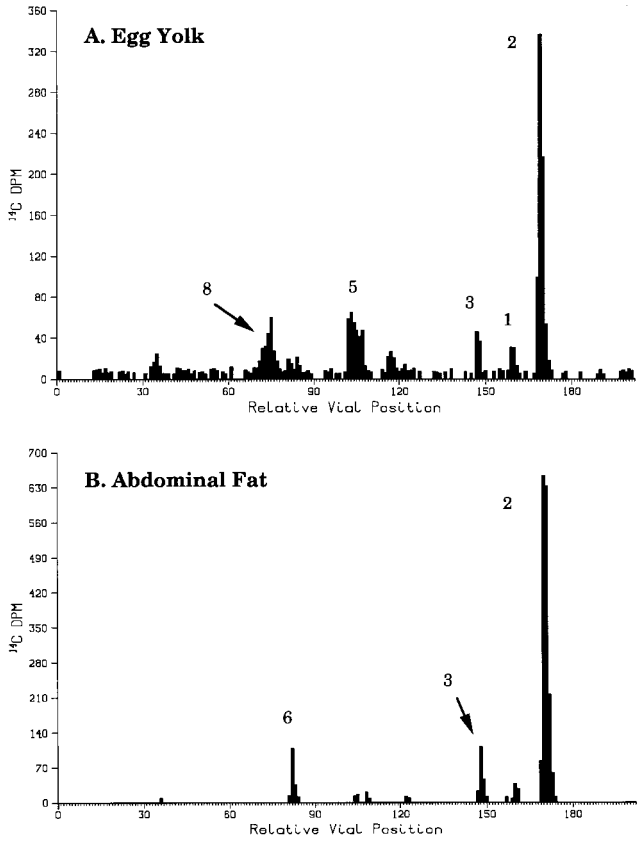

Figure 2. HPLC separation of thiazopyr and its metabolites isolated from (A) egg yolk and (B) abdominal fat. Vials were collected at 0.3 min intervals.

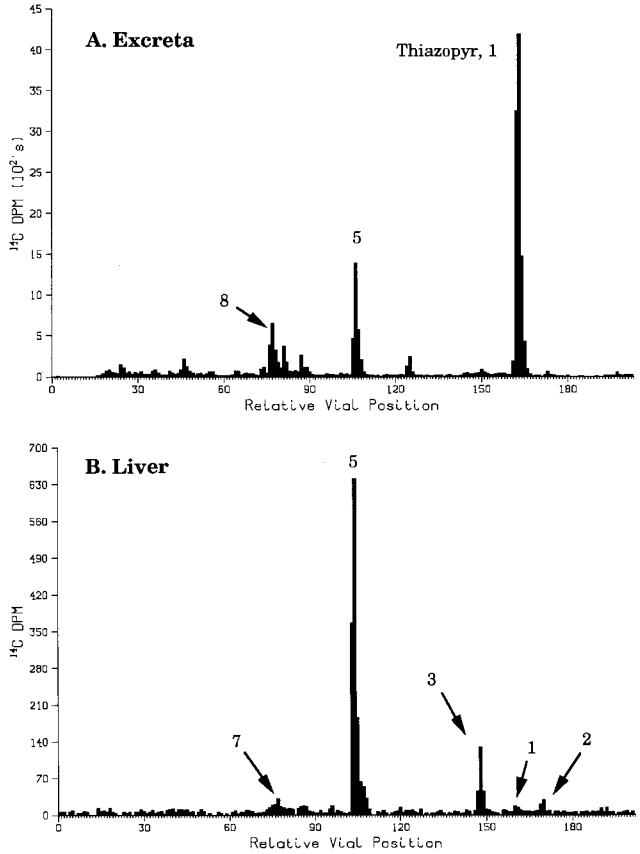

Figure 3. HPLC separation of thiazopyr and its metabolites isolated from (A) excreta and (B) liver. Vials were collected at 0.3 min intervals.

Representative HPLC profiles for the tissues and excreta are shown in Figures 2 and 3. Thiazopyr (**1**) was found to be a prominent component in the excreta, probably due to its poor absorption, and a very minor residue in the tissues analyzed. Samples of liver and egg yolk were fortified with thiazopyr, extracted, and analyzed by HPLC. The profiles indicated that thiazopyr was stable during the tissue extraction procedure.

Metabolite Identification. Seven hen metabolites were identified in this study and are illustrated in Figure 1. All metabolites were isolated from the tissues and excreta with the exception of metabolite **4**, which was identified as a liver metabolite of **2** in an in vitro reaction using hen liver homogenate.

Metabolite **2**, methyl 5-cyano-2-(difluoromethyl)-4-(2-methylpropyl)-6-(trifluoromethyl)-3-pyridinecarboxylate, and metabolite **3**, methyl 2-(difluoromethyl)-4-(2-methylpropyl)-5-(2-thiazolyl)-6-trifluoromethyl)-3-pryridinecarboxylate, were isolated from egg yolk, abdominal fat, and either skin with fat (**2**) or liver (**3**). The GC/CI/MS negative-ion spectrum for **2** from egg yolk is shown in Figure 4. The molecular weight was established as 336 on the basis of a cluster at *m/z* 336, 337 [M, M + 1]$^{\bullet -}$. The doublet arises from the 1:1 ratio of ^{12}C:^{13}C present in thiazopyr test material. The M + 2 ion at 338 is due to ^{14}C present in the high specific activity sample used for the low-dose groups.

Metabolite **3** gave a molecular ion at *m/z* 394, 395 [M, M + 1]$^{\bullet -}$ by GC/CI/MS (negative-ion) which was 2 amu lower than that for thiazopyr, suggesting oxidation somewhere in the molecule. Previous studies (Feng et al., 1994; Feng and Solsten, 1994) have demonstrated that the thiazoline ring is readily hydroxylated followed by dehydration to give the thiazole by rat liver microsomes, and therefore the thiazole structure was proposed for **3** as shown in Figure 1.

Metabolite **5**, methyl 4-(2-carboxypropyl)-5-cyano-2-(difluoromethyl)-6-(trifluoromethyl)-3-pyridinecarboxylate, was the major metabolite in the liver and a prominent metabolite in the excreta as shown in Figure 3. The excreta was used as the initial source of this metabolite to permit identification using MS and ^{1}H and ^{19}F NMR. The molecular weight for **5** was established as 366 by negative-ion FAB/MS as indicated by the doublet cluster at *m/z* 365, 366 [M − H, M + 1 − H]$^{-}$ (Figure 5). A mass of 365.0553 ($C_{14}H_{10}N_2O_4F_5^-$) was observed by high-resolution negative-ion FAB/MS, which was within 0.8 mmu of the calculated value. Derivatization of **5** with diazomethane and analysis by GC/CI/MS (positive-ion) gave the expected doublet at *m/z* 381, 382 [M + H, M + 1 + H]$^{+}$, which was observed due to an increase of 14 mass units resulting from the formation of the methyl ester derivative.

The 300 MHz ^{1}H NMR spectrum of **5** (Figure 6) was, while still containing some impurities, consistent with the structure proposed by mass spectral analysis. The 1:2:1 pattern with $J = 54$ Hz at δ 6.949−6.589 is due to the $-CF_2H$ group, and the singlet at δ 4.012 represents the hydrogens of the $-CO_2CH_3$ methyl ester. The resonances between δ 3.6 and 2.3 are due to the methylene and tertiary hydrogens of the isobutyl side chain, and the isobutyl methyl group appears as a doublet at δ 1.259 and 1.284. The assignments of the hydrogens of the isobutyl side chain for **5** were unambiguous due to the 500 MHz 2-D COSY spectrum shown in Figure 7. A cross-peak between the multiplet at δ 2.9 and the methyl group at δ 1.3 establishes this

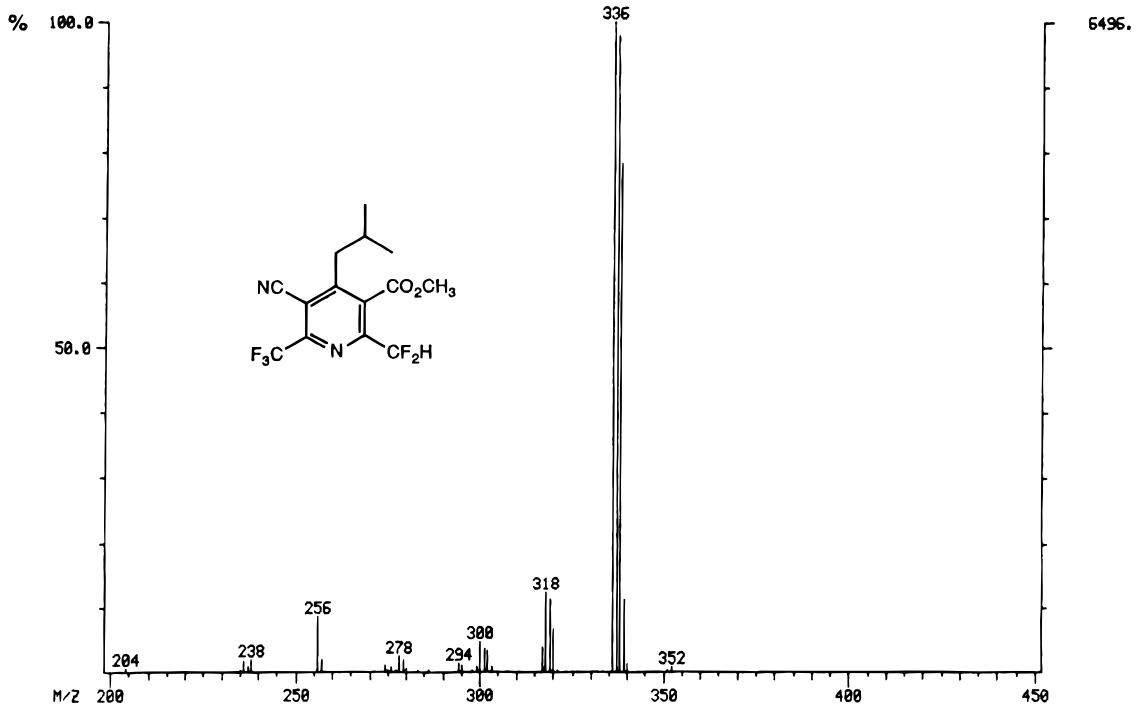

Figure 4. GC/CI/MS negative-ion spectrum of abdominal fat metabolite **2**.

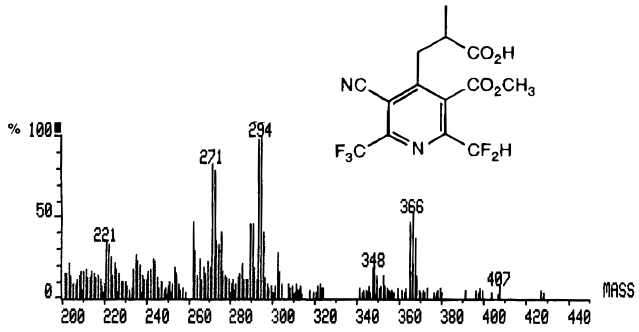

Figure 5. FAB/MS negative-ion spectrum of excreta metabolite **5**.

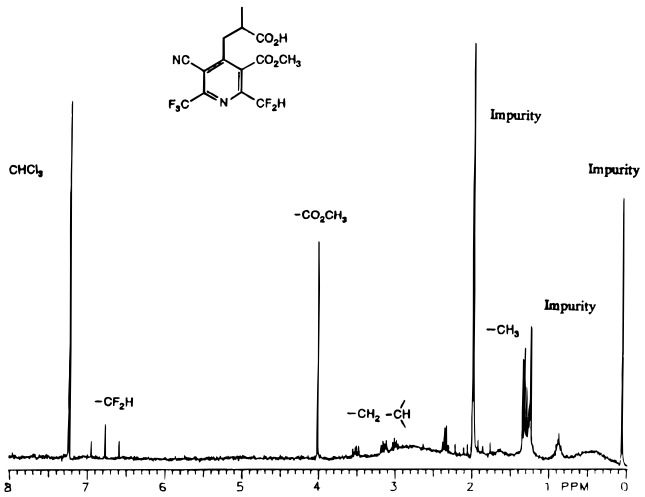

Figure 6. 300 MHz ^{1}H NMR of metabolite **5** isolated from excreta.

multiplet as corresponding to the methine hydrogen (H_b) in the isobutyl side chain. Cross-peaks were observed between this methine hydrogen and the two multiplets at δ 3.1 (H_{a1}) and δ 3.5 (H_{a2}), which correspond to the two benzylic hydrogens. Further coupling between these cross-peaks appears as the other cross-peak, confirming the diastereopic geminal relationship for the hydrogens. The benzylic hydrogens are prochiral and display distinct chemical shifts because of the anisotropic environment resulting from the adjacent chiral center. The 300 MHz ^{19}F NMR (not shown) demonstrated the presence of the $-CF_3$ group (δ -66.45) and the $-CF_2H$ group (multiplet between δ -117.2 and -117.8). The multiplet for the $-CF_2H$ group is due to the introduction of a chiral center in the isobutyl side chain generating a diastereotopic $-CF_2H$ group.

As shown in Figures 2 and 3, the retention time of metabolite **5** from the liver and egg yolk agreed with that observed for the excreta. Derivatization of **5** isolated from the tissue matrices with diazomethane and analysis by mass spectrometry (GC/CI/MS, negative-ion) established the molecular weight of the derivative as 380 in agreement with the results for the methyl ester.

The HPLC retention time for metabolite **6**, 8-(difluoromethyl)-3,4-dihydro-3,3-dimethyl-1-oxo-6-(trifluoromethyl)-1*H*-pyrano[3,4-*c*]pyridine-5-carbonitrile, did not match any existing standards, and attempts to derivatize it with diazomethane were unsuccessful, suggesting that the material did not contain a free carboxylic acid. Mass spectral analysis by GC/CI/MS (positive-ion) gave a doublet at *m*/*z* 321, 322 $[M + H, M + 1 + H]^+$ and established the molecular weight as 320. A weak doublet was observed in the positive-ion CI mass spectrum, which was consistent with the addition of reagent gas (isobutane) to the parent molecule and is characteristic of nitriles. LC/FAB (negative-ion) gave a doublet at *m*/*z* 320, 321 $[M, M + 1]^{\bullet -}$ that was consistent with the presence of a neutral molecule, because no proton elimination was observed. The nitrile lactone structure for **6** as shown in Figure 1 was proposed to account for the mass spectral and chemical derivatization data.

Metabolite **7**, methyl 5-(aminocarbonyl)-2-difluoromethyl)-4-(2-methylpropyl)-6-(trifluoromethyl)-3-pyridine-

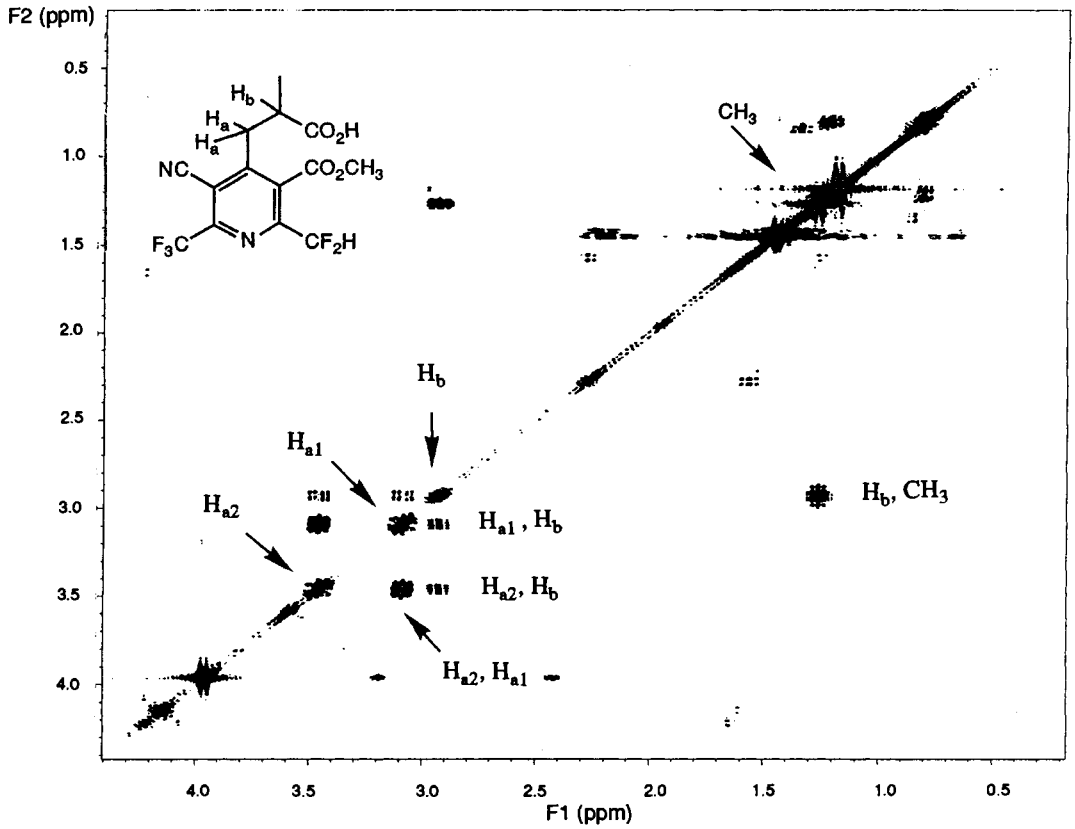

Figure 7. 500 MHz 2-D COSY ^{1}H NMR of metabolite **5** isolated from excreta.

5-carbonitrile, was isolated as a minor metabolite from the liver (Figure 3). The molecular weight of **7** was established as 354 by GC/CI/MS (negative-ion), and the spectrum was in agreement with that of an authentic standard.

Metabolite **8**, 5-cyano-2-(difluoromethy)-4-(2-methyl-1-propenyl)-6-(trifluoromethyl)-3-pyridinecarboxylic acid, was isolated from the excreta and egg yolk and analyzed by LC/FAB/MS (negative-ion). The molecular weight was established as 320 due to a doublet at *m/z* 319, 320 $[M - H, M + 1 - H]^-$, and the presence of a carboxylic acid group was indicated by a fragment ion at *m/z* 275, 276 $[M - CO_2H, M + 1 - CO_2H]^-$. Derivatization with diazomethane gave a molecular weight of 334 by GC/CI/MS (negative-ion), consistent with the formation of a methyl ester 14 mass units higher than the underivatized metabolite. The HPLC, mass spectral, and chemical derivatization results matched those obtained for an authentic standard of **8** and consistent with the structure proposed in Figure 1.

Quantitation of Residues in Tissues and Eggs. The levels of individual metabolites in the tissues and eggs of group 2 are shown in Table 3. Thiazopyr was shown to be rapidly metabolized and eliminated from hens, and this is reflected in the very low (<0.01 ppm) residues in all tissues examined. The highest metabolite residues were **2** in the abdominal fat (0.119 ppm) and **5** in the liver (0.122 ppm). All other metabolites were <0.06 ppm. The total unextracted residue was shown to be <0.1 ppm for all tissues.

In Vitro Metabolism of Metabolite 2 by Liver Homogenates. The in vitro metabolism of metabolite **2** by liver homogenates was studied to elucidate the metabolic pathways for thiazopyr and to provide an opportunity to compare the pathways of hens, goats, and rats. Sufficient quantities of **2** were isolated for the abdominal fat of group 3, and liver homogenates were prepared from control hens, goats, and rats as described under Materials and Methods. Incubation of **2** in the presence of an NADPH regenerating system and hen liver homogenate for 3 h followed by HPLC analysis gave the profile shown in panel A of Figure 8. A control incubation (not shown) using boiled liver homogenate incubated under identical conditions resulted in no metabolism of **2**. In vitro metabolites of **2** were tentatively assigned on the basis of their relative vial position and results of previous tissue analyses. To establish the identity of the peaks, the deproteinized supernatant

Table 3. Nature of Tissue Residues following Treatment with [^{14}C]Thiazopyr (1.3 mg/Day)

	tissue residue[a,b] (μg equiv/g)					
compound	egg yolk	liver	abdom fat	skin with fat	kidney	thigh muscle
thiazopyr, **1**	0.002	0.002	0.005	0.003	nd[c]	0.0001
metabolite **2**	0.018	0.004	0.119	0.057	0.001	0.0011
metabolite **3**	0.002	0.020	0.014	0.007	nd	0.0001
metabolite **5**	0.008	0.122	nd	0.004	0.029	0.0007
metabolite **6**	nd	nd	0.012	0.003	nd	0.0002
metabolite **7**	nd	0.008	nd	nd	0.002	0.0001
metabolite **8**	0.006	nd	nd	nd	nd	nd
unknowns	0.023	0.094	0.008	0.008	0.005	0.0041
total extracted	0.059	0.250	0.158	0.082	0.037	0.0064
unextracted	0.023	0.068	0.015	0.007	0.015	0.0013
% accountability	109	107	100	91.8	101	113

[a] Metabolite tissue residues were calculated by the following expression: tissue ppm × fraction of HPLC profile for individual metabolite × % of tissue activity in extract × 0.01 [b] Refer to Table 2, group 2, for tissue residue ppm values prior to extraction. The kidney and thigh muscle samples were composites of groups 1 and 2 and had initial values of 0.0517 and 0.0068 ppm, respectively. [c] nd, not detected.

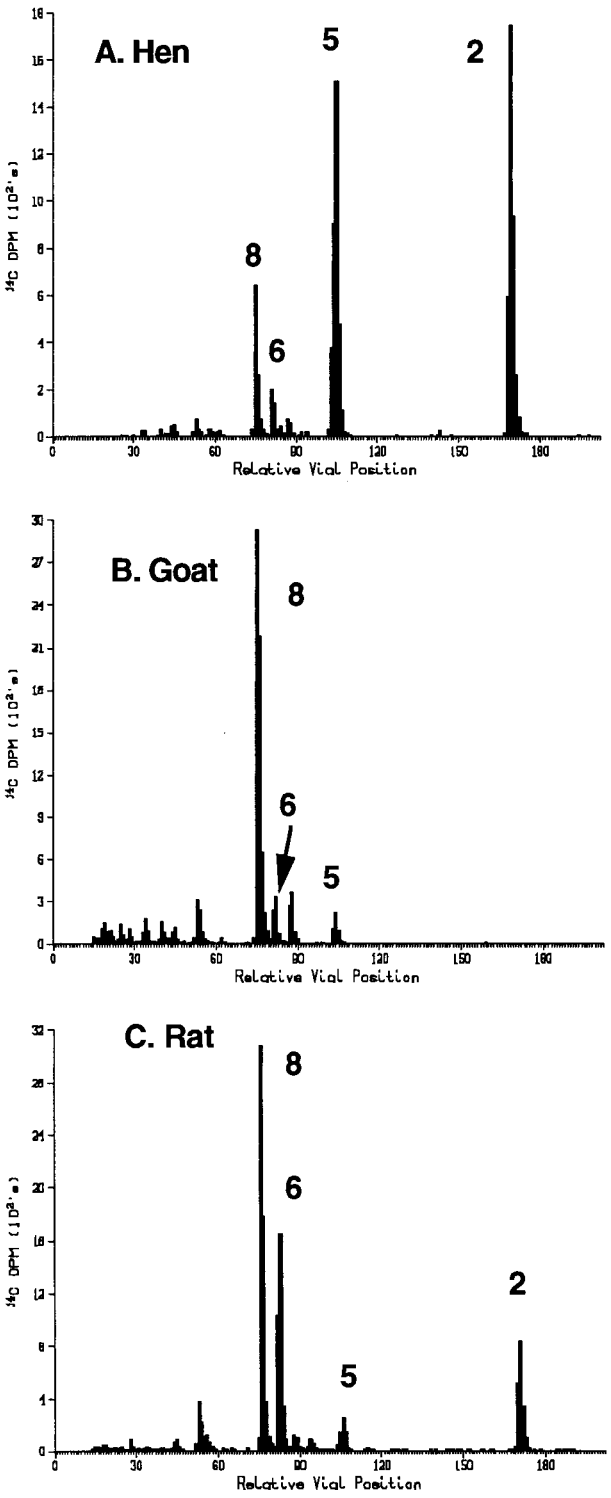

Figure 8. Comparative metabolism of nitrile ester metabolite **2** by liver homogenates.

of the hen in vitro reaction was acidified, extracted three times with an equal volume of methylene chloride, concentrated, and divided into two portions. One portion of the extract was derivatized with diazomethane, and then both the derivatized and underivatized portions were analyzed by GC/CI/MS (negative-ion). Unmetabolized **2** and metabolite **6** were identified in the underivatized sample on the basis of their molecular weights of 336 and 320, respectively. Metabolites **5** and **8** were identified in the derivatized sample on the basis of the molecular weights of 380 and 334, respectively, of their methyl ester derivatives.

A minor metabolite in the hen liver homogenate reaction was detected by mass spectral analysis of both the derivatized and underivatized samples. The molecular weight was established as 352 due to the presence of a doublet at *m/z* 352, 353 $[M, M + 1]^-$ in the mass spectrum and the tentative structure for metabolite **4**, methyl 5-cyano-2-(difluoromethyl)-4-[2(or 3)-hydroxy-2-methylpropyl]-6-(trifluoromethyl)-3-pyridinecarboxylate, shown in Figure 1, assigned. The location of the −OH in the isobutyl side chain could not be determined with the existing data. Metabolite **4** had not been identified in previous analyses of the tissues.

The rate of metabolism of **2** by goat and rat homogenates was found to exceed that of the hen as shown by a comparison of panels A−C in Figure 8. Similar metabolites were produced in all animals, but the levels of individual metabolites differed. The most significant metabolite in hen in vitro reaction was **5**, whereas in goat and rat metabolite **8** was predominant.

DISCUSSION

Thiazopyr was shown to be rapidly metabolized in hens, and this was reflected in the very low (<0.01 ppm) residues of the parent compound in all tissues examined (see Table 3). The identification of all metabolites at tissue levels of ≥0.01 ppm demonstrated that nitrile ester **2** was the most abundant metabolite in the abdominal fat, skin with fat, egg yolk, and thigh muscle. Metabolite **2** had been previously isolated from the metabolism of thiazopyr by rat liver homogenates (Feng et al., 1994; McClanahan et al., 1995) and shown to result from C- and S-oxidation of the thiazoline ring by either flavin or P450 monooxygenases. A second major metabolite, **5**, resulting from the oxidation of the isobutyl side chain was found in the liver and kidney. This metabolite had been previously isolated as a minor component from rat liver homogenates (McClanahan et al., 1995) and a structure proposed based on mass spectral data. The availability of larger quantitites of **5** isolated from the hen excreta permitted the detailed characterization of this metabolite by 2-D COSY ^{1}H NMR and ^{19}F NMR. All of the data are consistent with the oxidation of C-3 in the isobutyl side chain to a carboxylic acid. The resulting product contains a chiral center, and therefore the possibility exists for the stereoselective formation of only one enantiomer. Oxidation of the isobutyl side chain of atrazine by liver microsomes from rats, pigs, and humans demonstrated that the stereoselectivity of the products varied with species (Lang et al., 1996).

A comparison of the metabolism of **2** by liver homogenates from hens, goats, and rats (Figure 8) indicated that similar products were formed for all animals but the levels of individual metabolites varied. The most prominent in vitro metabolite for hen was **5**, in agreement with its relative abundance in the excreta and tissues following oral dosing. Alternatively, the unsaturated nitrile acid, **8**, was found to be the predominant in vitro metabolite for rats and goats.

A metabolic scheme for the formation of thiazopyr metabolites in the hen is shown in Figure 9. The thiazole ester **3**, amide ester **7**, and nitrile ester **2** are produced as a result of C- and S-oxidation of the thiazoline ring of thiazopyr as proposed by Feng et al. (1994) and McClanahan et al. (1995). Nitrile ester **2** is

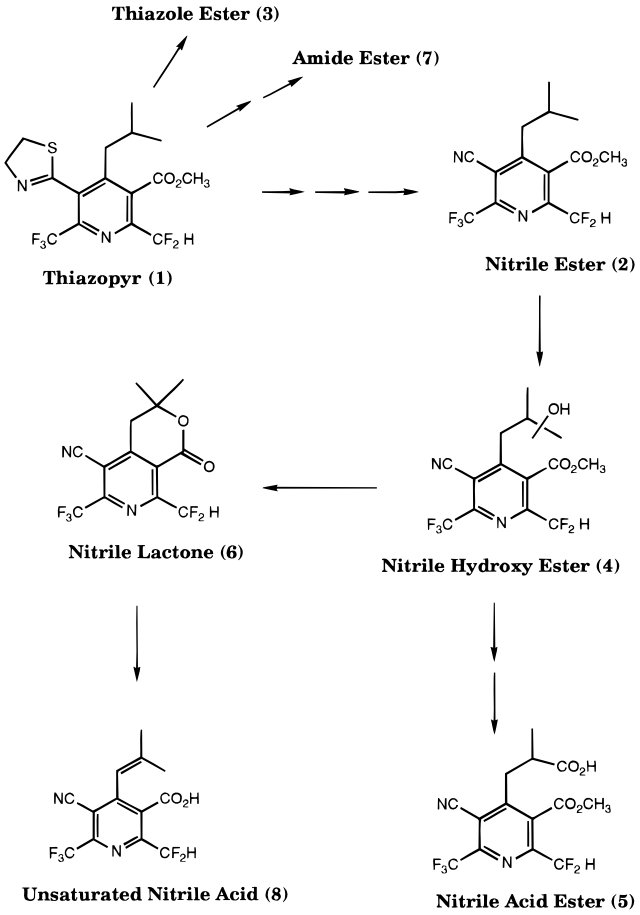

Figure 9. Metabolic pathways for thiazopyr.

then oxidized at either C-2 or C-3 to form a pair of alcohols. The in vitro formation of nitrile hydroxy ester **4** by hen liver homogenates is consistent with this step. Further oxidation of the C-3 alcohol results in the formation of the carboxylic acid of metabolite **5**. Alternatively, the C-2 alcohol can be converted to the six-membered lactone **6** and then hydrolyzed and dehydrated to form the unsaturated nitrile acid **8**. The relative contributions of metabolites **5** and **8** would be determined by the formation of C-3 or C-2 alcohols, respectively. In vitro data suggest that C-3 oxidation of **2** predominates in hen and C-2 oxidation is more prevalent in goats and rats.

ACKNOWLEDGMENT

We thank Dr. Sherry J. Logusch for her help in the collection and interpretation of the NMR data and Dr. Robert H. McClanahan for his advice and suggestions.

LITERATURE CITED

Armbruster, B. L.; Molin, W. T.; Bugg, M. W. Herbicide MON 7200 alters regulation of tubulin polymerization in wheat root tip cells. *Plant Physiol. Suppl*. **1988**, *86* (Abstract 583), 97.

Armbruster, B. L.; Molin, W. T.; Bugg, M. W. Effects of the herbicide dithiopyr on cell division in wheat root tips. *Pestic. Biochem. Physiol*. **1991**, *39*, 110−120.

Feng, P. C. C.; Solsten, R. T. In vitro biotransformation of thiazopyr by rat liver microsomes: oxidative cleavage of a carboxylic methylester by monooxygenases. *Xenobiotica* **1994**, *24*, 729−734.

Feng, P. C. C.; Solsten, R. T.; McClanahan, R. H. In vitro transformation of thiazopyr by rat liver enzymes: sulfur and carbon oxidations by microsomes. *Pestic. Biochem. Physiol*. **1994**, *48*, 8−14.

Feng, P. C. C.; Ruff, T. G.; Kosinski, W. G. Metabolic deactivation of the herbicide thiazopyr by animal liver esterases. *Xenobiotica* **1995a**, *25*, 27−35.

Feng, P. C. C.; Rao, S. R.; Schafer, D. E. Inhibition of thiazopyr metabolism in plant seedlings by inhibitors of monooxygenases. *Pestic. Sci*. **1995b**, *45*, 203−207.

Klemm, G. H.; Logusch, E. W.; Honegger, J. L.; Fujiwara, H.; Solsten, R. T.; McMullan, P. C. The metabolism of thiazopyr in Sprague−Dawley rats: characterization, identification, and distribution of thiazopyr and its metabolites following oral and intravenous administration. Presented at the 206th National Meeting of the American Chemical Society, Chicago, IL, Aug 1993; Poster AGRO 67.

Lang, D.; Criegee, D.; Grothusen, A.; Saalfrank, R. W.; Bocker, R. H. In vitro metabolism of atrazine, terbuthylazine, ametryne and terbutryne in rats, pigs and humans. *Drug Metab. Dispos*. **1996**, *24*, 859−865.

McClanahan, R. H.; Solsten, R. T.; Feng, P. C. C.; Logusch, E. W. In vitro metabolism of thiazopyr plant metabolites by rat liver enzymes. *Pestic. Biochem. Physiol*. **1995**, *51*, 90−98.

Rao, S. R.; Feng, P. C. C.; Schafer, D. E. Enhancement of thiazopyr bioefficacy by inhibitors of monooxygenases. *Pestic. Sci*. **1995**, *45*, 209−213.

Received for review March 17, 1998. Revised manuscript received July 1, 1998. Accepted July 7, 1998.

JF9802833